



Experimental Evaluation of the Effect of Incident Wave Frequency on the Performance of a Dual-chamber Oscillating Water Columns Considering Resonance Phenomenon Occurrence

R. Shafaghat*, M. Fallahi, B. Alizadeh Kharkeshi, M. Yousefifard

Sea-Based Energy Research Group, Babol Noshirvani University of Technology, Babol, Iran

PAPER INFO

Paper history:

Received 09 January 2022

Accepted in revised form 01 March 2022

Keywords:

Caspian Sea

Dual-chamber oscillating water column

Experimental study

Resonance frequency

Wave energy

ABSTRACT

This paper has experimentally investigated the performance of a dual-chamber oscillating water columns (OWC) imposed on Caspian Sea wave's characteristics. Experimental runs were performed for three water draft depths of 10, 15, and 20 cm and eight wave frequencies ranging from 0.4 to 0.7 Hz. Also, if the converter consists of only one chamber, the power generated was 75W; however, by placing the second chamber serial behind the first chamber, the converter power increased to 116 watts (55% improvements). The results showed that if the frequency of the incident wave is not in the natural frequency range, the converter performs is better at the lowest water draft depth (10 cm). Whereas if the frequency of the incident wave is in the natural frequency range, the converter will have the best performance at the maximum water draft depth (20 cm). As the power generated at a water draft depth of 10 cm increased by 3.8% compared to a water draft depth of 20 cm. But within the natural frequency range and by resonance, the power produced at a depth of 20 cm is 27.3% more than the power generated at a depth of 10 cm.

doi: 10.5829/ijee.2022.13.02.01

NOMENCLATURE

T	Period (s)	V	Velocity (m/s)
d	Draft depth (cm)	W_{owc}	Extractable power of OWC (W)
g	Gravitational acceleration (m/s ²)	W_w	Incident wave power (Watt)
H_{in}	Incident wave height (cm)	L	Wavelength (m)
h	water depth (m)	ρ	Density (kg/m ³)
k	wave number (rad/m)	ω	Incident wave frequency (Hz)
p	Pressure (Pa)	Abbreviation	
P_t	Output power (Watt)	RAO	Response Amplitude Operator
Q	Flow rate (m ³ /s)	WEC	Wave Energy Converter
u	Uncertainty (m)	OWC	Oscillating Water Column

INTRODUCTION

Today governments are looking to increase the supply of renewable energy sources to reduce the usage of non-renewable energy sources such as coal and oil. Reducing dependence on fossil fuels in the future is essential to solve climate change problems. Developing renewable

energy technologies is an alternative to ensure energy consumption without destroying the environment [1, 2].

Currently, about 19.3% of the world's energy consumption is renewable energy [3]. Among the various sources of renewable energies, ocean wave energy is a suitable source with high potential. Benefits such as high energy density, low environmental impact, and high

*Corresponding Author Email: rshafaghat@nit.ac.ir (R. Shafaghat)

reliability are the advantages of sea wave energy. Theoretical evaluations have shown that the total energy potential of the sea waves is 32,000 TWh/y, which is almost twice the amount of global electricity supply in 2008 [4]. In 2015, Reguero et al. [5] presented a new estimate of global potential energy (based on wave energy direction and global shoreline alignment). Potential sources are from 16,000 to 18,500 TWh/y, which is comparable to the global electricity consumption in 2016 (about 21,200 TWh/y).

Oscillating Water Columns (OWC) are wave energy converters with a simple structure as a great advantage; Also, a large part of the industrial wave energy converters are OWC [6]. The OWC is one of the most common wave energy converters that has been the subject of research and development for decades. Various geometries have been introduced for this converter till now. Among them, the dual-chamber OWC had a better performance compared to the single-chamber OWCs [7].

Boccotti [8] compared the U-shaped and rectangular OWCs and showed that the U-shaped model performed better than the rectangular model. The U-shaped OWC has a larger natural period than the rectangular model; also performs much better in large and small wave conditions. Dorrell et al. [9] analyzed and tested a three-chamber OWC. They implemented a turbine to extract energy and modeled water fluctuations inside the chambers using the Runge Kutta (RKN) method. He et al. [10] investigated the hydrodynamic performance of a multi-chamber OWC in two modes (single-chamber and multi-chamber). The results showed that a multi-chamber OWC performs better than a single-chamber OWC. Hsieh et al. [11] developed a wave energy converter using a dual-chamber OWC for a specific site on the east coast of Taiwan. In the mentioned study, sea wave characteristics and OWC size were modeled with the help of landing scaling. The results showed that the dual-chamber OWC performed better than the single-chamber OWC. Wilbert et al. [12] experimentally investigated the interaction of a wave with dual-chamber OWC, the effect of wave height on efficiency was investigated; Experiments were also performed to simulate a single-chamber OWC without a front duct and to understand the impact of the front channel. Martinelli et al. [13] studied a multi-chamber OWC according to the wave characteristics of the Mediterranean Sea; The OWC was called Seabreath. The relationship between incident wave height and free surface fluctuations was determined during experimental tests. Due to the choice of Orifice and small channel, the system efficiency was lower than expected. Nielsen and Bingham [14] Experimental tests were performed on a multi-chamber device (KNSWING) to achieve energy from the OWC. The results showed that when the wave height is 5 meters, the converter can generate 2.5 MW of power; Also, the efficiency of the device was measured in wave conditions with medium periods between 5 to 7 seconds and with a significant wave height of 2 meters,

20 to 25%. Rezanejad et al. [15] investigated the performance of a dual-chamber OWC by placing a step on the floor of the OWC. The results showed that the dual-chamber with steps has a much better performance than the single-chamber OWC. Shalby et al. [16] studied a fixed structure multi-chamber OWC. The system was tested under different incident wave conditions and geometry changes. The results showed that the multi-chamber OWC performs well on a large scale. Rezanejad et al. [17] investigated the performance of a near-shore dual-chamber OWC. The effects of separation wall distance and length on the performance of OWC have been studied. The results showed that the dual-chamber OWC has a much better performance. He et al. [18] investigated the performance of a dual-chamber OWC; they showed that if the incident wave frequency is equal to the natural frequency of the converter, the OWC performs better in absorbing wave energy. Also, the wave frequency was more effective than the other parameters among the incident wave characteristics.

Incident wave characteristics are crucial in studying the performance and hydrodynamic behavior of an OWC. Since the Caspian Sea is considered the goal sea, some studies on the Caspian Sea are mentioned below. In 2013, Rusu and Onca [19] analyzed the energy of the Caspian Sea wave; they showed that this sea could be considered as a strategic source of power in the future. In 2013, Fadaee Nejad et al. [20] studied the energy potential of the Caspian Sea waves on Tonekabon coast. Some studies have demonstrated that wave energy could reach up to 9 kWh in offshore areas.

In 2014, Hadadpour et al. [21] studied the Caspian Sea wave characteristics of Anzali. They showed that the wave height must reach 2 meters to achieve maximum efficiency, and its period must reach 4 to 7 seconds. In 2014, Alamian et al. [22] studied and analyzed the energy potential of the waves of the entire Caspian Sea. They evaluated different types of energy converters to find the optimal one. In another study in 2017, Alamian et al. [23] investigated the energy potential of waves on the southern shores of the Caspian Sea and extracted important wave characteristics in these areas.

Past studies have shown that the frequency of incident waves has a significant effect on the performance of OWC (single-chamber and multi-chamber). The critical point is that the converter's efficiency will decrease sharply by increasing the incident wave's frequency [24]. For this reason, finding solutions to increase efficiency at high frequencies is essential. One of the effective ways to increase the efficiency at high frequencies is to place the natural frequency of the converter in the range of the incident wave frequency. In this case, if the frequency of the incident wave is equal to the natural frequency of the converter, due to the resonance phenomenon, it is possible to prevent a drastic decrease of efficiency in this frequency domain, which improves the performance of the system in this range of the incident wave frequency.

On the other hand, the study of the characteristics of the waves of the Caspian Sea as a target sea shown that this sea, unlike open seas, has high-frequency waves [23]. Therefore, in this study, a dual-chamber OWC imposed to Caspian sea wave characteristics by considering the resonance phenomenon has been experimentally investigated. According to the concept of the OWC, the incident wave causes reciprocating movement of the free surface inside the converter. The amplitude of these fluctuations can indicate the hydrodynamic response of the system to the incident wave. The hydrodynamic behavior of the OWC could be described by parameters such as RAO, the pressure inside the chamber, output air velocity of the air ducts, wave height inside the chamber, and the wave frequency produced by the wavemaker. Experimental tests were performed using a model converter with a scale of 1:10 in the wave tank. In this regard, by keeping the height of the incident wave constant, experimental tests were performed at eight frequencies and three draft depths. The converter behavior was also studied in two different frequency ranges. In the first step, experimental tests were carried out at frequencies outside the natural frequency range. In the next step, the converter performance was evaluated at frequencies close to the natural frequency of the converter.

MATERIALS AND METHODS

System description

According to the EMEC standard, five phases are defined for developing a converter from the initial idea to commercialization. The initial concept is confirmed in the first and second phases while evaluating the wave energy converter on a small scale [24–26]. Therefore, a dual-chamber OWC with a rectangular geometric shape was constructed (Figure 1). Each chamber has a length of 0.75 meters, a width of 0.60 meters, and a height of 1 meter. The whole OWC was placed on supports with a height of 0.80 m. In the upper part of the OWC, two high-pressure and low-pressure air ducts were installed, with a length of

1.5 meters and a width and height of 0.15 meter. Check valves were applied to enter and exit the airflow in these channels. These valves are a square shape with a length of 0.10 meter. The valves were also made of Plexiglas to be light and durable and open and close easily, and the OWC structure is made of iron to withstand waves.

The location of the converter in the wave tank and the physical model condition are shown in Figure 2. A pressure sensor and a wave gauge sensor were placed on the top of each chamber, and a velocity meter was used to record the inlet and output air velocities of the low and high-pressure air ducts. The dual-chamber OWC in the role of a breakwater was placed at the end of the wave tank. The distance from the converter to the wavemaker was 9.5 meters.

Target sea

The Caspian Sea has been selected as the target sea to install a dual-chamber OWC power plant (Figure 3). According to the studies of Alamian et al. [23], Babolsar port was chosen for the construction of OWC in terms of wave characteristics and the establishment of necessary infrastructure, including breakwater and tourism. The characteristics of the waves of the Caspian Sea in the port of Babolsar are shown in Figure 4. Wave's period and height are considered between 4-6 seconds and 0.5-1 meter as conditions of waves with the highest energy. However, the occurrence of these conditions also covers 23% of the year's hours. The Froude scale was used to convert the actual wave conditions to a laboratory scale.

Dimensional analysis and equations

With the help of dimensional analysis, it can be shown that the system's power depends on the dimensionless groups of the following equation:

$$C_p = \frac{P_{MOWC}}{\rho \omega^3 h^3} = f\left(\frac{\omega^2 h}{g}, \frac{d}{h}, \frac{H_{inc}}{h}\right) \quad (1)$$

C_p is the power coefficient, P_{MOWC} is the power of the dual-chamber OWC, ρ is the water density, ω is the frequency of the incident wave, h is the water depth, g is the gravity, d is the water draft depth, H_{inc} is the wave

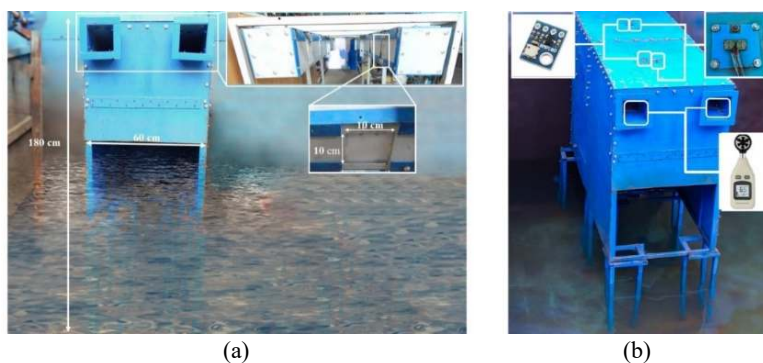


Figure 1. The OWC in the wave-tank

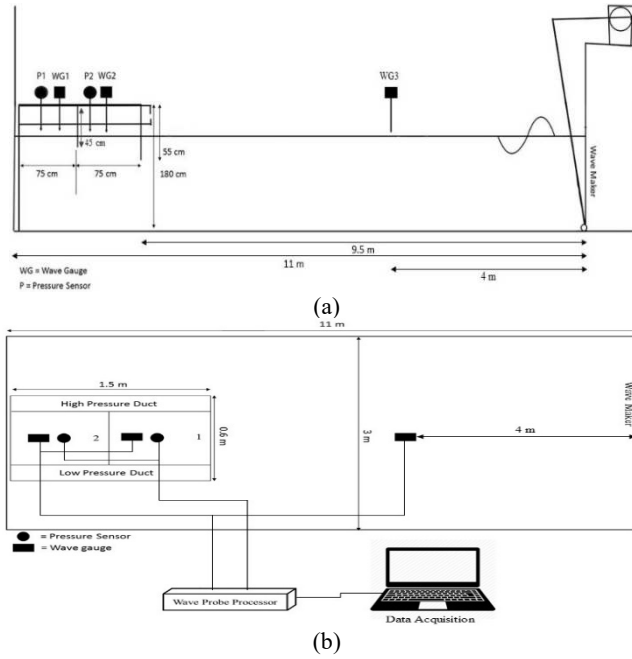


Figure 2. Test components from the (a) side and (b) top view and the locations



Figure 3. Caspian Sea and Babolsar shore location

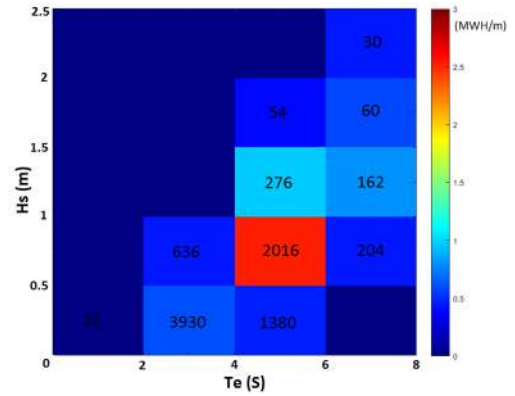


Figure 4. Diagram of the possibility of occurrence and density of wave energy in terms of significant wave height and wave period for Babolsar coast [23]

height inside the chamber, H_{inc} is the incident wave height. To investigate the efficiency of the converter, the input wave energy must be calculated using the following equations.

$$P_w = Ec_g \quad (2)$$

$$E = \frac{1}{2} \rho g L H^2 \quad (3)$$

$$C_g = \frac{\omega}{2k} \left(1 + \frac{2kh}{\sinh(2kh)} \right) \quad (4)$$

$$\omega^2 = kg \times \tanh(kh) \quad (5)$$

P_w is the power of the incident wave, E is the total wave energy in a period, and C_g is the group velocity of the wave. Also, to study each chamber's output power, the velocity and volumetric flow rate can be calculated by

considering the rigid piston theory and measuring the amplitude of oscillations inside the converter [16]. Then, having the volume flow rate and the results obtained from the pressure sensor, the output power of each chamber is calculated. With the output power of each chamber, the efficiency and Response Amplitude Operator (RAO) are obtained [27].

$$\eta = \frac{H}{2} \sin \omega t \quad (6)$$

$$\frac{\partial \eta}{\partial t} = V = \frac{H}{2} \omega \cos \omega t \quad (7)$$

$$Q = V_{MAX} A = \frac{H}{2} \omega A \quad (8)$$

$$P_{OWC} = \frac{H}{2} \omega A \times \Delta P \tag{9}$$

$$\epsilon = \frac{P_{MOWC}}{P_w} \tag{10}$$

$$RAO = \frac{H_{in}}{H_{in_{cin}}} \tag{11}$$

η Is free surface level inside the converter, V is free surface velocity, A is surface area, ΔP is the amplitude of Pressure fluctuations, ϵ is efficiency, and RAO is the hydrodynamic response of the system. Also, in Equation (9), the wave power coefficients with Betz coefficient (0.3) [24] are given.

The resonance phenomenon occurs when the incident wave frequency is equal to the natural frequency of the OWC. By the occurrence of this resonance phenomenon, the performance of the OWC device tends to be maximized. In this regard, the associated angular frequency can be estimated to be approximately by Equation (12) [28]:

$$\omega_N = \sqrt{\frac{g}{a + 0.41\sqrt{s}}} \tag{12}$$

where S is the sectional area of the OWC chamber. Hence, the resonant angular frequency of the studied OWC is predicted.

Experimental design

This study considered three draft depths and eight frequencies to study the effect of draft depth and frequencies on the dual-chamber OWC performance (see Table 1). Wave gauge and pressure sensors were installed on the top of the device separately to measure pressure wave height inside the chambers and calculate power and efficiency. 120 tests were performed on the dual-chamber OWC.

The procedure for conducting experimental studies is shown in Figure 5. As can be seen, first, according to the period of the waves of the Caspian Sea and scale of 1:10, frequency of incident waves is obtained. After adjusting the frequency, the required height of the wave is calculated. According to the located sensors, data acquisition is performed several times to satisfy the

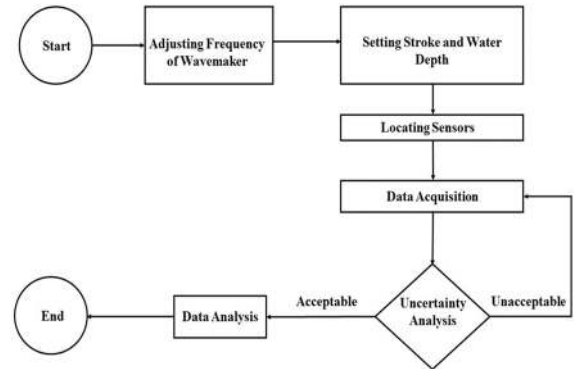


Figure 5. Flowchart of the data acquisition process

uncertainty analysis criteria. Finally, if the data is acceptable, they are used; however, the experiments are repeated if they are not accepted.

Laboratory equipment and measuring instruments

The sea-based energy research group's wave tank in Babol Noshirvani University of Technology was used(Figure 6). This wave tank has a length of 11 meters, a width of 3 meters, and a height of 3 meters and can produce regular waves in a wide range of height and period characteristics of waves. Also, its wavemaker system is flap-type (Figure 7). The wavemaker system is designed with a 5.5 kW motor, a reduced gearbox, and an inverter to adjust the output speed from zero to 150 rpm.

Output air velocity from orifices with the help of GM816A velocity-meter, the free surface fluctuation was measured using a US-100 ultrasonic sensor, and pressure changes were measured by a BMP-180 piezoresistive sensor (Table 2).



Figure 6. Left and right view of the wave tank in the Sea-Based Energy Research Group






Figure 7. Wavemaker and the components

Table 1. Classification of test conditions

Incident wave height (cm)	Draft depth (cm)	Frequency (Hz)							
		0.4	0.45	0.5	0.55	0.6	0.65	0.7	0.75
10	10	0.4	0.45	0.5	0.55	0.6	0.65	0.7	0.75
	15	0.4	0.45	0.5	0.55	0.6	0.65	0.7	0.75
	20	0.4	0.45	0.5	0.55	0.6	0.65	0.7	0.75

Table 2. Measurement instruments

Measuring instruments	Accuracy	Device	Image
velocity meter (GM816A)	0.1 m/s	velocitymeter	
Ultrasonic sensor (US-100)	3 mm	Wave gauge sensor	
BMP-180 Pressure Sensor	0.7% Pa	Pressure sensor	

Calibration and uncertainty analysis

Equipment calibration and test data uncertainty analysis are necessary to obtain reliable data and validate the measured values. As mentioned in this study, two wave gauges, two pressure sensors, and one velocity meter were implemented. Figure 8 shows the calibration system of wave gauges. The system consists of a pump, a tank, a drain valve, a camera, and a transparent cylindrical indicator. Wave gauge sensors are installed at the top of the tank for evaluation and calibration. The tank is filled to a certain level by the pump to start the calibration procedure. A transparent indicator is installed in one of the tank's sidewalls to record the trend of the water level decrease. The lower drain valve of the tank is opened to start the calibration, and the camcorder records the reduction in the water level. The data recorded by the wave gauge sensor is used to evaluate the sensor's calibration with the results extracted from the film. The calibration coefficient of the wave gauge sensors is obtained and is equal to 0.97.

A low-speed wind tunnel is applied to calibrate the pressure sensor (Figure 9). First, wind speed is measured by a velocity meter; after measuring the air velocity, the airflow pressure is calculated (using Bernoulli equation). The measured pressure is then compared with the pressure calculated from the Bernoulli equation, and the pressure sensor is calibrated.

After calibrating the measuring instrument, the data obtained from the tests were analyzed for uncertainty. Due to the high volume of uncertainty data analysis, In this section, it is sufficient to provide the required relations and velocity and pressure test data for a draft depth and a frequency as an example. Equations (13) to (16) have been applied to calculate the measurement uncertainty.

$$\bar{x} = \frac{\sum_{i=1}^n x_i}{n} \tag{13}$$

$$s = \sqrt{\frac{\sum_{i=1}^n (x_i - \bar{x})^2}{(n - 1)}} \tag{14}$$

$$u = \frac{s}{\sqrt{n}} \tag{15}$$

$$U = ku_c \tag{16}$$

Equation (13), \bar{x} is the average value, x_i is the parameter desired in each experiment, and n is the number of experiments. According to the tests carried out, each test was repeated five times to achieve a reliable level of results. In relation 14, s is the standard deviation, and in relation 15, u is the mean uncertainty. In Equation (16), U is a combined uncertainty with an overlap coefficient k . If k is considered equal to 2, the assuredness level of the results will reach 95%. An example of a velocity meter uncertainty analysis is shown in Figure 10; As it turns out, the data have an acceptable level of reliability, and the deviation from the results criterion is also acceptable.

RESULTS AND DISCUSSION

In the results section, the effect of changing incident wave frequency and draft depth on a dual-chamber OWC in the form of RAO, chamber pressure, output power, and efficiency were studied. In this regard, paying attention to the natural frequency of the converter can be very important; if the frequency of the incident wave is equal to the natural frequency of the converter, the resonance



Figure 8. Using tank, camera, and ruler to calibrate the wave gauge sensor

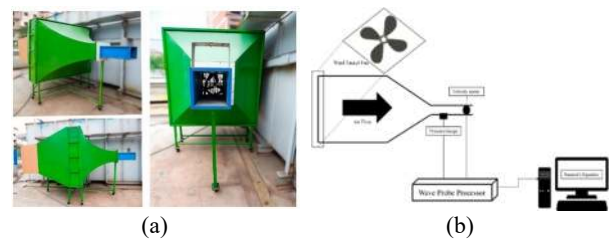


Figure 9. Using wind tunnel for velocity meter calibration

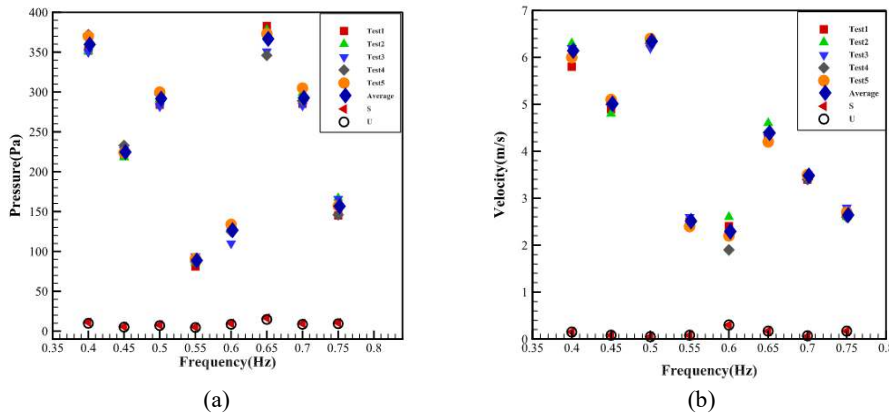


Figure 10. Uncertainty analysis of the results of measuring velocity and pressure for a draft depth of 10 cm

phenomenon can have a significant effect on the performance of the converter. It is also considering that the performance evaluation of each of the chambers in the dual-chamber converter helps to make more accurate evaluations. Therefore, studying the overall performance of the dual-chamber converter, effect of incident wave conditions on the first and second chambers were investigated in more detail.

Variations of RAO, pressure, and power in terms of incident wave frequency in the first and second chambers of the converter are shown in Figure 11. According to the figure, with an increase in the incident wave frequency in both chambers, two different behaviors were observed in the two frequency ranges [0.4-0.55] and [0.55-0.75]. Considering that the natural frequency of the converter (0.65 Hz) is in the frequency range [0.55-0.75], As the frequency of the incident wave approached the natural frequency of the converter, the system had a nonlinear behavior. Due to the resonance phenomenon, the RAO, pressure, and power will have a maximum value in all draft depths. However, in the frequency range [0.4-0.55] for all draft depths, a decreasing trend is observed for RAO, pressure, and power.

In the frequency range [0.4-0.55], the converter performs better at a draft depth of 10 cm compared to the other two draft depths. Since a unique natural phenomenon does not occur in this frequency range, and as draft depth decreases, the radiation wave decreases, and the incident wave enters the converter straightforwardly. Therefore, in these conditions, the converter performance in lower draft depth has better performance. However, in the frequency range [0.55-0.75], the converter has improved performance at a depth of 20 cm, Since there is more water inside the converter chamber in this frequency range when draft depth is more. Due to the higher inertia, the pressure inside the tank during the resonance phenomenon and, consequently, the output power increases more. In the case of chamber number 2, the same behavior is seen with chamber number 1. But the rate of sensitivity to draft depth in this

chamber is lower since chamber number 1 is exposed to a stronger wave.

Data on the simultaneous effect of incident wave frequency and draft depth on the converter output power are studied (Figure 12). The converter output power changes for the frequency ranges [0.4-0.55] and [0.55-0.75] are shown in Figures 12a and 12b, respectively. As mentioned, in the frequency range [0.5-4.5], the output power of the dual-chamber OWC decreases by increasing the frequency of the incident wave. While in the frequency range [0.55-0.75] due to the resonance phenomenon. Furthermore, increasing the incident wave frequency does not necessarily reduce the converter power.

In this case, the converter's power increases by raising the incident wave's frequency to the natural frequency range of the converter. By further increasing the frequency of the incident wave to values larger than the natural frequency, increasing the frequency leads to a decrease in power. In practice, it can be observed that being in the natural frequency range can be functionally desirable. On the other hand, according to the provided contours, for the frequency range [0.4-0.55], the draft depth does not significantly affect the output power of the converter. However, for the frequency range [0.55-0.75], increasing draft depth to 20 cm leads to a rise in the output power of the converter. Therefore, it is necessary to pay attention to the resonance frequency range to determine the optimum draft depth.

By measuring the airflow velocity of the ducts, the efficiency of the dual-chamber oscillating water column converter can be calculated. In this regard, according to the air velocity, first, considering the Betz coefficient of 0.25, the output power of the dual-chamber converter was calculated. Therefore, the converter's efficiency is obtained by calculating the output power of the dual-chamber converter and considering the incident wave power (Figure 13). According to the Figure, the maximum efficiency of the dual-chamber converter is 79.75%. On the other by froud scaling method, it could

be said that the converter generates 116 W at the best condition. By scale 1:10, the commercialized converter could generate 370 kW power at the best operation mode or 3241200 kWh per year.

In order to investigate each chamber's role in power generation, by having the pressure of each chamber and calculating the output flow of them (using the Bernoulli equation), the power generation of each chamber is calculated. Due to the specificity of the incident wave power, the efficiency of the first chamber is 52.72%. In other words, the first chamber has a share of 66.11% of the two-chamber converter's total capacity,

while the second chamber's share is 33.89% of the total capacity.

Therefore, due to the high importance of the first chamber, the efficiency changes of first chamber with frequency are shown in Figure 13. On the other hand, as one of the most important results, it can be said that as the frequency of the incident wave increases, the converter's efficiency decreases almost linearly. However, by reaching the natural frequency range and occurring resonance phenomenon at high frequencies, a relative increase in power and efficiency is again observed. These changes are more evident in the first chamber.

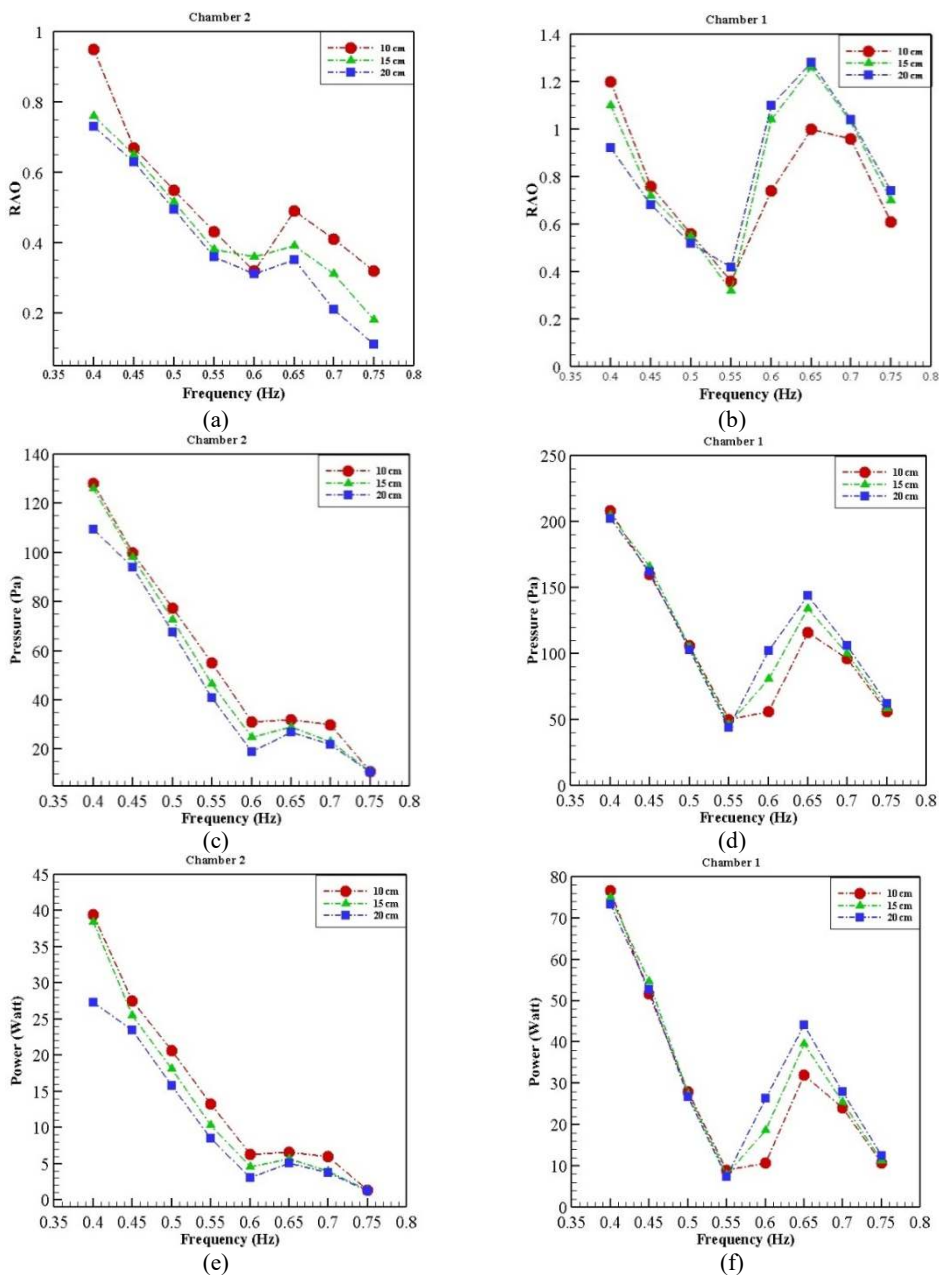


Figure 11. RAO variations, pressure, and power in chambers

As it has been stated, in the range outside the natural frequency, the draft depth does not affect efficiency, as the power generated at a draft depth of 10 cm increases by 3.8% compared to a water draft depth of 20 cm. However, in the natural frequency range and through resonance, the power generated at a depth of 20 cm is 27.3% more than the depth of 10 cm. In order to study the effect of water draft depth on the hydrodynamic

response of the system at the resonance frequency, the amplitude of free water level fluctuations and the pressure inside chamber one are shown in Figure 14. As it is known, the fluctuations of the free surface and the pressure inside the chamber at the resonant frequency for the draft depth of 20 cm are far more than the water draft depth of 10 cm, which can be a better choice for installing the device.

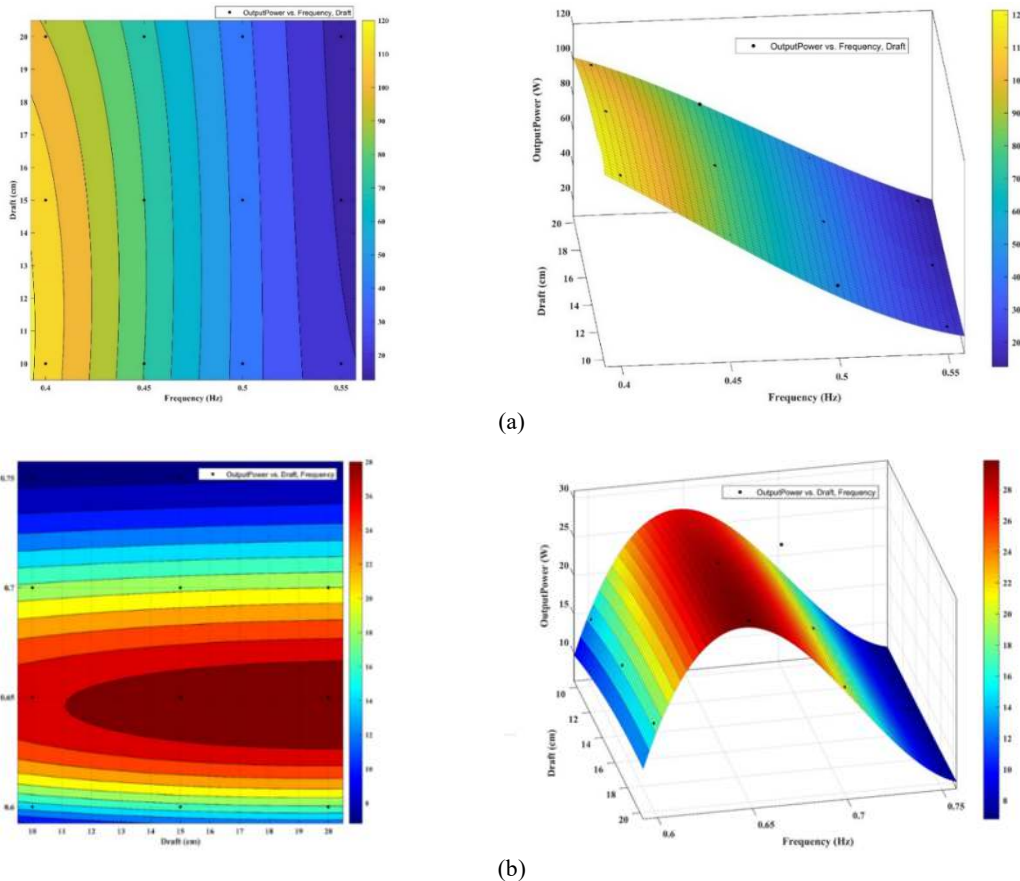


Figure 12. Power changes with frequency and draft depth for a) frequency range [0.4-0.55] frequency range [0.55-0.75]

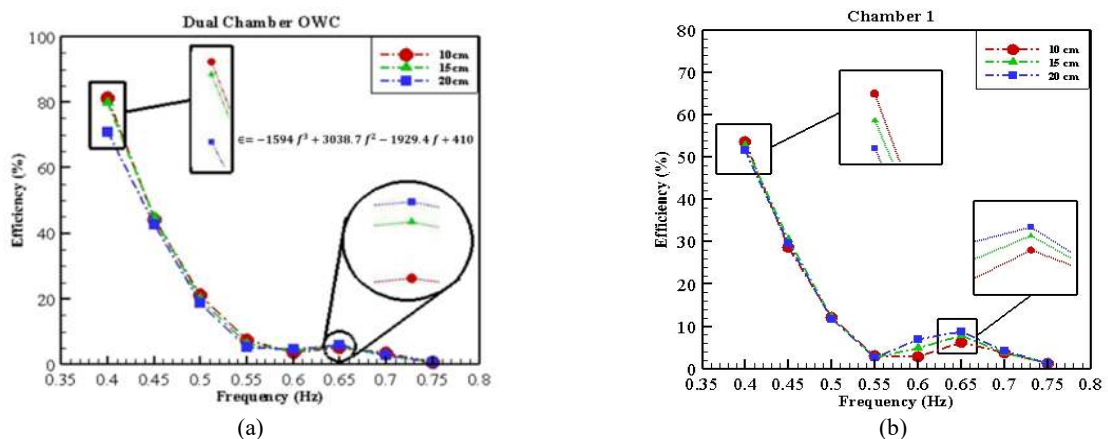


Figure 13. Efficiency variations of the first chamber and dual chamber converter with frequency

In order to evaluate the effect of dimensionless groups on the performance of the system, power coefficient variation by draft depth in the dimensionless frequencies of the incident wave have been investigated (Figure 15). According to the figure, the power coefficient has a higher value at low dimensional frequencies. Of course, it is worth noting that power variations with draft depth are also much larger at low frequencies. By increasing the draft depth in the dual-chamber OWC, the power coefficient at the lowest dimensionless frequency (0.023) decreases by 13.3%. To observe in more detail, the contribution of the first chamber in reducing the power coefficient is also shown in Figure 15. As can be seen, by increasing dimensionless draft depth, the first chamber at the lowest dimensionless frequency has a significant power coefficient reduction of 22.7%. To justify this phenomenon, as the draft depth increases, the radiation wave from the first chamber is much stronger than the second chamber; Therefore, the portion of power coefficient loss in this chamber is higher. On the other

hand, it can be said: at the lowest dimensionless frequency and draft depth, the converter power coefficient of the dual-chambers is 1.51 times the power coefficient of the first chamber.

Considering that the incident wave frequency in the sea changes continuously, to investigate the overall performance of the converter, the average efficiency at different frequencies for the dual-chamber converter and the first chamber has been calculated (Figure 16). Obviously, for better evaluation of the average efficiency, the maximum efficiency is also shown in Figure 16. According to the figure, considering the maximum efficiency, the first chamber has generated an average of 68.17% of the total efficiency of the dual-chamber converter. Considering the average efficiency, the portion of the first chamber is equal to 71.01% of the total efficiency of the dual-chamber converter. This result shows that the first chamber plays a significant role in generating power, even for average and maximum efficiency.

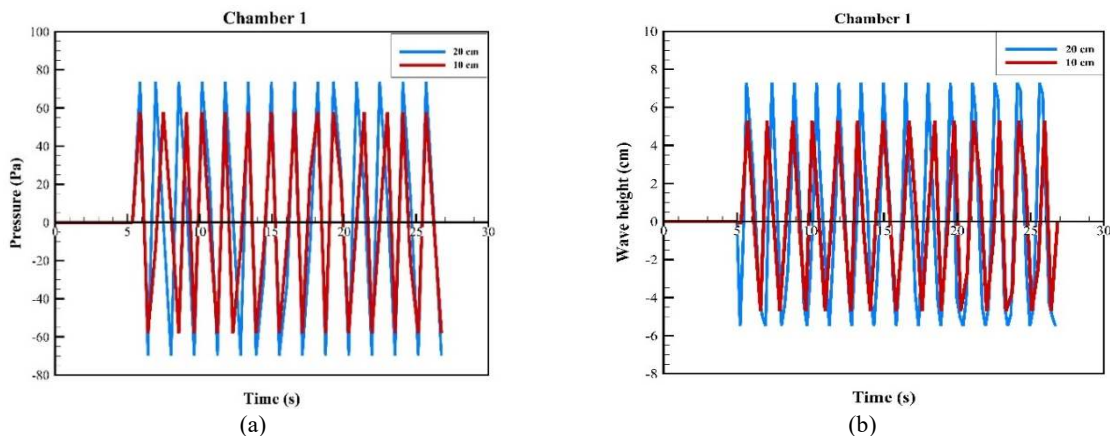


Figure 14. Comparison of free surface fluctuations and pressure inside chamber 1 at the resonance frequency for draft depths of 10 and 20 cm

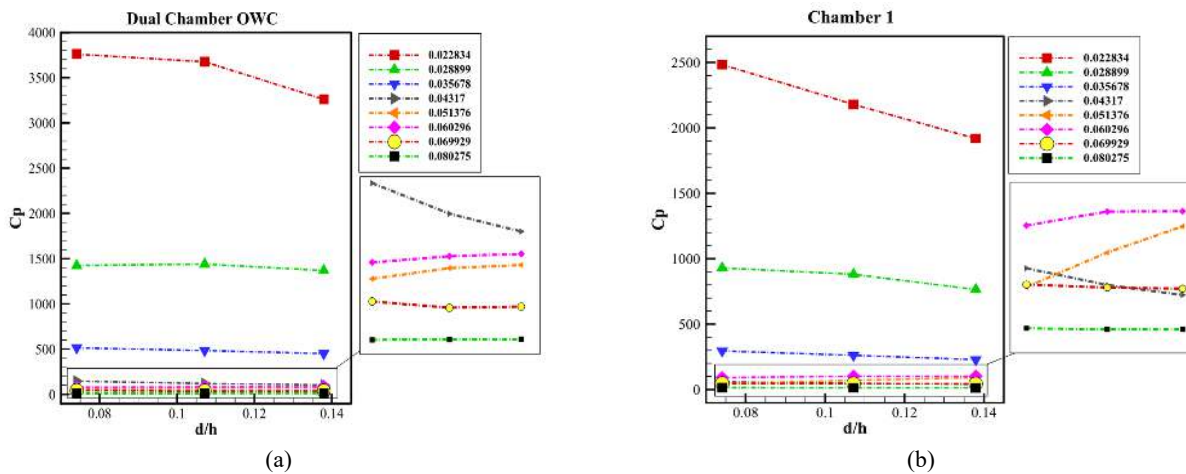


Figure 15. Variations in the power coefficient of chamber No. 1 and the whole converter with the frequency

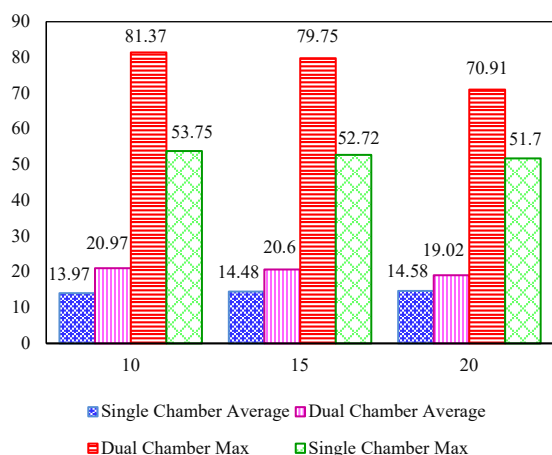


Figure 16. Comparison of average and maximum efficiency for two ranges

CONCLUSION

This paper has studied a dual-chamber fixed structure oscillating water column with nonlinear PTO imposed to Caspian Sea wave conditions experimentally. hydrodynamic behavior of OWC depends on frequency of the incident wave. In such a way, if the frequency of the incident wave is equal to the natural frequency of the converter. The resonance phenomenon improves the performance of the OWC. The system response to the incident wave was evaluated using parameters such as frequency of the incident wave, amplitude of fluctuations and the pressure inside the chamber, the output power, and the efficiency. To achieve important results, experimental tests were performed for eight incident wave frequencies and three draft depths. The most significant achievements of this research include the following:

- Increasing the frequency of the incident wave leads to a decrease in the efficiency of the converter sharply. Therefore, if the natural frequency of the converter is in the range of the incident wave frequency during the low-efficiency interval, the resonance phenomenon changes the linear decreasing behavior of the converter to the nonlinear response and increases the efficiency; relative increase in efficiency improves the performance of the converter.
- Considering that the Caspian Sea wave frequency is much higher than the high seas, applying this strategy in the range of the Caspian Sea wave has improved the converter performance at high frequencies of the incident wave.
- The power and efficiency of the dual-chamber OWC have been calculated by considering the Betz coefficient of 0.25. The maximum pneumatic efficiency of the dual-chamber converter and the first chamber were 79.75% and 52.72%, respectively;

which shows that the first chamber has 66.11% of the total capacity of the dual-chamber converter; while, the share of the second chamber is 33.89% of the total capacity .

- Investigation of the effect of draft depth has shown that in the range outside the natural frequency, the draft depth has no significant effect on efficiency. As the power produced at a draft depth of 10 cm increases by 3.8% compared to a draft depth of 20 cm. However, in the natural frequency range and by resonance, the power generated at a depth of 20 cm is 27.3% more than the power generated at a depth of 10 cm.
- By increasing the draft depth in the dual-chamber OWC, the power coefficient at the lowest dimensionless frequency (0.023) decreases by 13.3%; the first chamber accounts for a larger share of the power coefficient reduction. The power coefficient reduces by about 22.7% by increasing the dimensionless draft depth in these conditions. Also, at the lowest dimensionless frequency and draft depth, the dual-chamber system has a power coefficient of 1.51 times the power coefficient of the first chamber.
- Calculation of average pneumatic efficiency and maximum pneumatic efficiency at different frequencies for the dual-chamber converter and the first chamber shows that the first chamber has produced an average of 68.17% of the total efficiency of the dual-chamber converter by considering the maximum efficiency. For average efficiency, the portion of the first chamber is equal to 71.01% of the total efficiency of the dual-chamber converter. This result shows that the first chamber plays a significant role in generating power, even for average and maximum efficiency.

REFERENCES

1. Brooke, J., 2003. Wave energy conversion. Elsevier, <https://www.elsevier.com/books/wave-energy-conversion/brooke/9780-08-044212-9>
2. McCormick, M.E., 2013. Ocean wave energy conversion. Courier Corporation, <https://doi.org/10.1016/C2016-0-01219-6>
3. Sawin, J.L., Sverrisson, F., Rutovitz, J., Dwyer, S., Teske, S., Murdock, H.E., Adib, R., Guerra, F., Blanning, L.H., and Hamirwasia, V., 2018. Renewables 2018-Global status report. A comprehensive annual overview of the state of renewable energy. Advancing the global renewable energy transition-Highlights of the REN21 Renewables 2018 Global Status Report in perspective, https://inis.iaea.org/search/search.aspx?orig_q=RN:49053208
4. Mofk, G., Barstow, S., Kabuth, A., and Pontes, M.T., 2010. Assessing the Global Wave Energy Potential. In: 29th International Conference on Ocean, Offshore and Arctic Engineering: Volume 3. ASME, pp 447-454, <https://asmigitalcollection.asme.org/OMAE/proceedings/OMA E2010/49118/447/345942>
5. Reguero, B.G., Losada, I.J., and Méndez, F.J., 2015. A global wave power resource and its seasonal, interannual and long-term

- variability. *Applied Energy*, 148, pp.366–380. Doi: 10.1016/j.apenergy.2015.03.114
6. Falcão, A.F.O., and Henriques, J.C.C., 2016. Oscillating-water-column wave energy converters and air turbines: A review. *Renewable Energy*, 85, pp.1391–1424. Doi: 10.1016/j.renene.2015.07.086
 7. Shalby, M., Dorrell, D.G., and Walker, P., 2019. Multi-chamber oscillating water column wave energy converters and air turbines: A review. *International Journal of Energy Research*, 43(2), pp.681–696. Doi: 10.1002/er.4222
 8. Boccotti, P., 2007. Comparison between a U-OWC and a conventional OWC. *Ocean Engineering*, 34(5–6), pp.799–805. Doi: 10.1016/j.oceaneng.2006.04.005
 9. Dorrell, D.G., Hsieh, M.-F., and Lin, C.-C., 2010. A Multichamber Oscillating Water Column Using Cascaded Savonius Turbines. *IEEE Transactions on Industry Applications*, 46(6), pp.2372–2380. Doi: 10.1109/TIA.2010.2072979
 10. He, F., Huang, Z., and Wing-Keung Law, A., 2012. Hydrodynamic performance of a rectangular floating breakwater with and without pneumatic chambers: An experimental study. *Ocean Engineering*, 51, pp.16–27. Doi: 10.1016/j.oceaneng.2012.05.008
 11. Min-Fu Hsieh, I-Hsien Lin, Dorrell, D.G., Ming-June Hsieh, and Chi-Chien Lin, 2012. Development of a Wave Energy Converter Using a Two Chamber Oscillating Water Column. *IEEE Transactions on Sustainable Energy*, 3(3), pp.482–497. Doi: 10.1109/TSSTE.2012.2190769
 12. Wilbert, R., Sundar, V., and Sannasiraj, S.A., 2013. Wave Interaction with a Double Chamber Oscillating Water Column Device. *The International Journal of Ocean and Climate Systems*, 4(1), pp.21–39. Doi: 10.1260/1759-3131.4.1.21
 13. Martinelli, L., Pezzutto, P., and Ruol, P., 2013. Experimentally Based Model to Size the Geometry of a New OWC Device, with Reference to the Mediterranean Sea Wave Environment. *Energies*, 6(9), pp.4696–4720. Doi: 10.3390/en6094696
 14. Nielsen, K., and Bingham, H., 2015. MARINET experiment KNSWING testing an I-Beam OWC attenuator. *International Journal of Marine Energy*, 12, pp.21–34. Doi: 10.1016/j.ijome.2015.08.005
 15. Rezanejad, K., Bhattacharjee, J., and Guedes Soares, C., 2015. Analytical and numerical study of dual-chamber oscillating water columns on stepped bottom. *Renewable Energy*, 75, pp.272–282. Doi: 10.1016/j.renene.2014.09.050
 16. Shalby, M., Walker, P., and Dorrell, D.G., 2016. The investigation of a segment multi-chamber oscillating water column in physical scale model. In: 2016 IEEE International Conference on Renewable Energy Research and Applications (ICRERA). IEEE, pp 183–188, Doi: 10.1109/ICRERA.2016.7884534
 17. Rezanejad, K., Bhattacharjee, J., and Guedes Soares, C., 2016. Analytical and Numerical Study of Nearshore Multiple Oscillating Water Columns. *Journal of Offshore Mechanics and Arctic Engineering*, 138(2), pp.1–16. Doi: 10.1115/1.4032303
 18. He, F., Leng, J., and Zhao, X., 2017. An experimental investigation into the wave power extraction of a floating box-type breakwater with dual pneumatic chambers. *Applied Ocean Research*, 67, pp.21–30. Doi: 10.1016/j.apor.2017.06.009
 19. Rusu, E., and Onea, F., 2013. Evaluation of the wind and wave energy along the Caspian Sea. *Energy*, 50, pp.1–14. Doi: 10.1016/j.energy.2012.11.044
 20. Fadaee Nejad, M., Shariati, O., and Mohd Zin, A.A. Bin, 2013. Feasibility study of wave energy potential in southern coasts of Caspian Sea in Iran. In: 2013 IEEE 7th International Power Engineering and Optimization Conference (PEOCO). IEEE, pp 57–60, Doi: 10.1109/PEOCO.2013.6564515
 21. Hadadpour, S., Etemad-Shahidi, A., Jabbari, E., and Kamranzad, B., 2014. Wave energy and hot spots in Anzali port. *Energy*, 74, pp.529–536. Doi: 10.1016/j.energy.2014.07.018
 22. Alamian, R., Shafaghat, R., Miri, S.J., Yazdanshenas, N., and Shakeri, M., 2014. Evaluation of technologies for harvesting wave energy in Caspian Sea. *Renewable and Sustainable Energy Reviews*, 32, pp.468–476. Doi: 10.1016/j.rser.2014.01.036
 23. Alamian, R., Shafaghat, R., Hosseini, S.S., and Zainali, A., 2017. Wave energy potential along the southern coast of the Caspian Sea. *International Journal of Marine Energy*, 19, pp.221–234. Doi: 10.1016/j.ijome.2017.08.002
 24. Alizadeh Kharkeshi, B., Shafaghat, R., Alamian, R., and Aghajani Afghan, A.H., 2020. Experimental & Analytical Hydrodynamic Behavior Investigation of an Onshore OWC-WEC Imposed to Caspian Sea Wave Conditions. *International Journal of Maritime Technology*, 14, pp.1–12, <http://dorl.net/dor/20.1001.1.23456000.2020.14.0.5.0>
 25. Sanaye, S., and Katebi, A., 2014. 4E analysis and multi objective optimization of a micro gas turbine and solid oxide fuel cell hybrid combined heat and power system. *Journal of Power Sources*, 247, pp.294–306. Doi: 10.1016/j.jpowsour.2013.08.065
 26. Alizadeh Kharkeshi, B., Shafaghat, R., Jahanian, O., Rezanejad, K., and Alamian, R., 2021. Experimental Evaluation of the Effect of Dimensionless Hydrodynamic Coefficients on the Performance of a Multi-Chamber Oscillating Water Column Converter in Laboratory Scale. *Modares Mechanical Engineering*, 21(12), pp.823–834. <http://dorl.net/dor/20.1001.1.10275940.1400.21.12.5.5>
 27. Shalby, M., Walker, P., and Dorrell, D.G., 2017. Modelling of the multi-chamber oscillating water column in regular waves at model scale. *Energy Procedia*, 136(2), pp.316–322. Doi: 10.1016/j.egypro.2017.10.261
 28. Rezanejad, K., Guedes Soares, C., López, I., and Carballo, R., 2017. Experimental and numerical investigation of the hydrodynamic performance of an oscillating water column wave energy converter. *Renewable Energy*, 106(2), pp.1–16. Doi: 10.1016/j.renene.2017.01.003

COPYRIGHTS

©2021 The author(s). This is an open access article distributed under the terms of the Creative Commons Attribution (CC BY 4.0), which permits unrestricted use, distribution, and reproduction in any medium, as long as the original authors and source are cited. No permission is required from the authors or the publishers.



Persian Abstract

چکیده

مبدل‌های گوناگونی برای استحصال انرژی امواج دریا پیشنهاد شده‌اند که از جمله مبدل‌های پربازده می‌توان به ستون‌های نوسانی آب اشاره نمود. عملکرد ستون‌های نوسانی آب وابستگی زیادی به شرایط امواج دریا دارد. در این راستا مشخصه‌های امواج برخوردی و عمق آبخور تأثیر به‌سزایی بر راندمان و عملکرد مبدل خواهد داشت. در این مقاله، عملکرد یک ستون نوسانی دومحفظه‌ای تحت شرایط امواج دریای مازندران مورد ارزیابی تجربی قرار گرفته است. آزمون‌های تجربی در استخر موج انجام شدند و مقیاس مدل آزمایشگاهی ۱:۱۰ در نظر گرفته شد. پس از کالیبراسیون تجهیزات و آنالیز عدم قطعیت، مطالعات برای سه عمق آبخور ۱۰، ۲۰ و ۳۰ سانتی‌متر و نیز برای هشت فرکانس موج در محدوده‌ی ۰/۴ تا ۰/۷۵ هرتز انجام شد. ارتفاع موج برخوردی در همه‌ی آزمون‌ها ثابت فرض شد. با توجه به نتایج، پاسخ هیدرودینامیکی مبدل به فرکانس طبیعی سامانه وابسته است؛ به‌طوری‌که اگر فرکانس موج برخوردی در محدوده‌ی فرکانس طبیعی سامانه نباشد، با افزایش فرکانس، راندمان به‌صورت خطی کاهش می‌یابد؛ اما برای حالتی که فرکانس موج برخوردی در محدوده‌ی فرکانس طبیعی سامانه قرار دارد، با افزایش فرکانس، راندمان مبدل در ابتدا افزایش و سپس کاهش می‌یابد. همچنین اگر مبدل تنها از یک محفظه تشکیل شده باشد، توانی معادل ۷۵ وات تولید می‌نماید؛ اما با قرار دادن محفظه‌ی دوم به‌صورت سری در پشت محفظه‌ی اول، توان مبدل تا ۱۱۶ وات (۵۵٪) افزایش می‌یابد. نتایج بررسی عمق آبخور نشان می‌دهد که اگر فرکانس موج برخوردی در محدوده‌ی فرکانس طبیعی نباشد، مبدل در کمترین عمق آبخور (۱۰ سانتی‌متر) عملکرد بهتری دارد. در حالی که اگر فرکانس موج برخوردی در محدوده‌ی فرکانس طبیعی باشد، مبدل در بیشترین عمق آبخور (۲۰ سانتی‌متر) بهترین عملکرد را خواهد داشت. شایان‌ذکر است که در محدوده‌ی خارج از فرکانس طبیعی، عمق آبخور تأثیر زیادی بر راندمان ندارد. به‌گونه‌ای که توان تولیدشده در عمق آبخور ۱۰ سانتی‌متر در مقایسه با عمق آبخور ۲۰ سانتی‌متر، ۳/۸٪ افزایش می‌یابد؛ اما در محدوده‌ی فرکانس طبیعی و به‌واسطه‌ی رزونانس، توان تولیدشده در عمق آبخور ۲۰ سانتی‌متر ۲۷/۳٪ بیشتر از توان تولیدشده در عمق آبخور ۱۰ سانتی‌متر می‌باشد.
